Study on the Phase Transition Behavior of Poly(butylene adipate) in its Blends with Poly(vinyl phenol)

ARTICLE *in* THE JOURNAL OF PHYSICAL CHEMISTRY B · FEBRUARY 2011

Impact Factor: 3.3 · DOI: 10.1021/jp110003m · Source: PubMed

THE JOURNAL OF PHYSICAL CHEMISTRY B

ARTICLE

pubs.acs.org/JPCB

Study on the Phase Transition Behavior of Poly(butylene adipate) in its Blends with Poly(vinyl phenol)

Xiaoli Sun,[†,‡] Fuwei Pi,[†] Jianming Zhang,[§] Isao Takahashi,[†,*] Feng Wang,[‡] Shouke Yan,[‡,*] and Yukihiro Ozaki[†]

[†]School of Science and Technology, Kwansei Gakuin University, Sanda, Hyogo 669-1337, Japan;

[‡]State Key Laboratory of Chemical Resource Engineering, Beijing University of Chemical Technology, Beijing 100029, China;

[§]Key Laboratory of Rubber-plastics, Ministry of Education, Qingdao University of Science and Technology, Qingdao City 266042, China.

ABSTRACT: The phase transition behavior of poly(butylene adipate) (PBA) crystals in its blends with poly(vinyl phenol) (PVPh) was investigated by infrared (IR) spectroscopy and X-ray diffraction (XRD). The IR and XRD studies indicate that the hydrogen bonding between the C═O group of PBA and the OH group of PVPh developed in the PBA/PVPh blends with the ratios of 80/20 and 50/50 does not influence the solution crystallization behavior of PBA. The phase transition behavior of PBA in the blends is, however, significantly altered by the blending. In the neat PBA, linear changes of the intensities of IR bands at 1077, 930, and 910 cm^{-1} are observed in the temperature range of 25−47.5 °C followed by an abrupt change corresponding to the occurrence of β-to-α phase transition. In the blends, the accelerated intensity changes of the those IR bands occur before the β-to-α phase transition, which is contributed to the melting of imperfect β-PBA crystals at relatively lower temperature. In addition, the significantly depressed β-to-α phase transition temperature is also identified.

INTRODUCTION

In recent years, biodegradable polymeric materials have received considerable attention owing to their environmental and ecological advantages. However, some disadvantages of biodegradable polymers, such as poor biocompatibility, poor processability, and weak mechanical properties, limit their applications greatly. Thus, different modification ways have been developed for tailoring the mechanical properties and degradation kinetics of biodegradable polymers to suit for various applications.[1−3] Among many others, blending a biodegradable polymer with another composition for improving its properties is a much easier and faster way compared to other modification methods. For blend systems, numerous efforts have been made to minimize the interfacial energy and reduce the propensity of phase separation of the polymers by using compatibilizers or introducing reactive groups to covalently connect individual polymers.[4,5] The use of a hydrogen bonding to improve interfacial properties is particularly appealing because of the potential for relatively low process temperature and mixing at the molecular level.[6−16] Because of the existence of the hydroxyl group in poly(vinyl phenol) (PVPh), as shown in Scheme 1, which readily leads to a specific hydrogen bonding interaction, PVPh has attracted tremendous interest in the preparation of novel polymer blends. A number of investigations have proved that PVPh exhibits excellent miscibility benefiting from the hydrogen bonding with biodegradable polymer, such as poly(hydroxy alkanoates) and aliphatic polyesters.[17−22]

Poly(butylene adipate) (PBA) (Scheme 1) is a biodegradable polymorphic materials, which has two types of crystal forms, that is, thermodynamically most stable α-form and kinetically favorable β-form.[23,24] Previous studies demonstrated that the α and β PBA crystals exhibit different physical properties and biodegradability.[25] Consequently, studies on the formation mechanism and phase transition behavior of the PBA from its β-crystals to its α-counterparts have recently received considerable attention.[26,27] For such kinds of polymorphic biodegradable polymer, the formation of intermolecular hydrogen bonding may not only modify the phase separation of the blends but also alter the modification of crystals or/and influence the phase transition behavior. This, in turn, influences its mechanical and thermal performances as well as biodegradability. Therefore, there is a special interest of gaining more knowledge of the phase behavior of these kinds of blends. However, a great amount of studies have been carried out only on the miscibility and resultant morphologies. Less attention has been paid to the phase transition behavior of PBA in its blend systems with hydrogen bonding interaction. This is actually of great importance for modifying the physicomechanical and biodegradable properties.

It is well documented that Fourier-transform infrared spectroscopy (FTIR) is very sensitive to the conformation and local molecular environment of a polymer. More specifically, responses of variations in segmental conformations and chain packing to temperature can be followed by monitoring changes in different IR characteristic bands. In the present study, the blend system of PBA and PVPh was selected and the structural evolutions of PBA in its blends with PVPh upon heating process have been investigated by IR spectroscopy and X-ray diffraction (XRD). The results show that blending PBA with PVPh alters the phase transition behavior of PBA significantly. Besides the depression of β-to-α phase transition temperature, multistage alterations of

Received: October 19, 2010
Revised: January 17, 2011
Published: February 14, 2011

Scheme 1

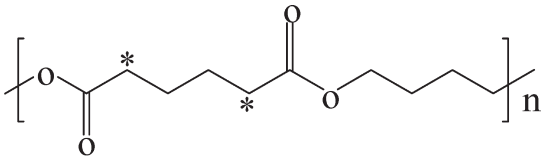

Chemical structure of Poly(butylene adipate)

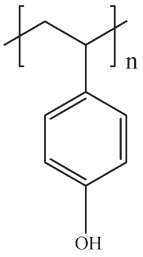

Chemical structure of Poly(vinyl phenol)

the intensities of IR bands at 1077, 930, and 910 cm^{-1} are observed in the PBA/PVPh blends with the ratios of 80/20 and 50/50. By analysis of the crystallization sensitive bands, the response of conformational dynamics to temperature has been explored.

EXPERIMENTAL SECTION

Materials and Preparation Procedures. Bacterially synthesized PBA (M_w = 12 000 g mol^{-1}) was purchased from Aldrich Cop. It was purified by dissolving in hot chloroform, precipitated in methanol, and vacuum dried at 60 °C. PVPh with the glass transition temperature of 105 °C was purchased from Aldrich Cop. and used without further purification. PBA/PVPh blends were prepared by dissolving them together in tetrahydrofuran (THF) with three different blending ratios, PBA/PVPh = 100/0, 80/20, and 50/50. Samples for IR and X-ray measurements were prepared by casting the solution with a concentration of 1% (w/v) on a KBr window and silicon wafer, respectively. After the majority of solvent had been evaporated, the resultant films were placed under vacuum at room temperature for 48 h to completely remove the residual solvent.

FTIR Measurement. The KBr window with the sample was set on a Linkman temperature cell, which had been placed in the sample compartment of a Thermo Nicolet Magna 470 spectrometer equipped with an MCT detector. The pristine cast sample was heated at a rate of 1 °C/min up to 80 °C. IR spectra of the specimen were collected at a 2 cm^{-1} resolution continuously during heating process. The spectra were obtained by adding 32 scans. During data analysis, the IR spectra were subjected to a linear baseline correction, followed by offsetting to the zero absorbance value. The crystalline bands were normalized in the following way:

$$(A_t - A_\infty)/(A_0 - A_\infty)$$

Where A_0, A_∞ and A_t represent the peak area at initial, melting and measured temperatures, respectively. For the amorphous bands, same normalization method was used with the position of A_0 and A_∞ in the equation being interconversed.

X-ray Diffraction. X-ray diffraction was used to characterize the crystallization status and crystalline structure of pure PBA and the PBA in the blends. The measurements were conducted on a high-resolution four-circle diffractometer with rotating-anode X-ray generator (SLX-2000 & UltraX, Rigaku Co., Ltd., X-ray wavelength = 0.15405 nm). The size of the incident beam was defined by a collimator with diameter of 2 mm. A soller slit was placed before a scintillation detector to collimate the scattered beam. The fixing time for data collection was 50 s per step, and the angular interval was 0.01°.

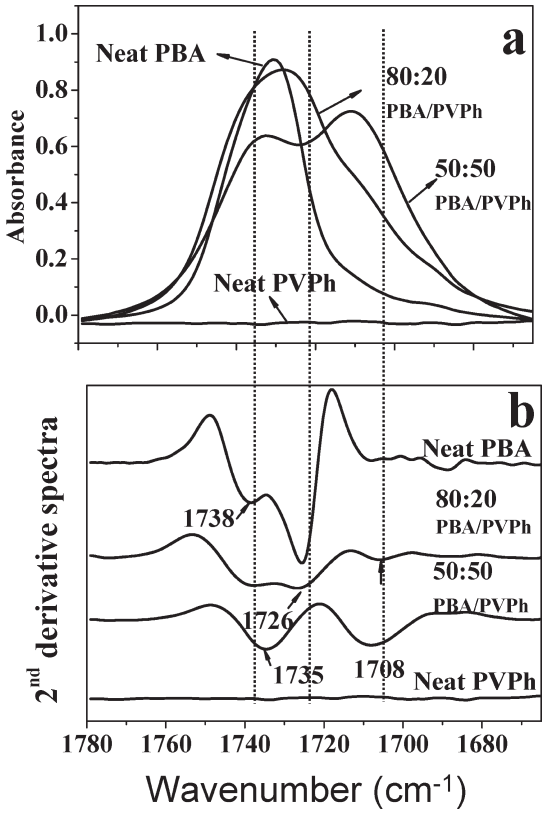

Figure 1. IR spectra in the C═O stretching band region of neat PBA, 80/20, and 50/50 blends with PVPh, and neat PVPh (a) and their second derivative spectra (b).

RESULTS AND DISCUSSION

Parts a and b of Figure 1 depict the IR spectra and their second derivatives respectively in the carbonyl stretching band region of the solution cast 100/0, 80/20, 50/50 and 0/100 PBA/PVPh films measured at room temperature. As can be seen in Figure 1, the PVPh film does not show any band in this region. The band assignment of the PBA is summarized in Table 1. Clearly, the carboxyl stretching bands of PBA show remarkable changes with the incorporation of PVPh component. From the second derivatives (part b of Figure 1), two major bands of the neat PBA are observed at 1738 and 1726 cm^{-1}, which are assigned to the carbonyl stretching bands of the amorphous and crystalline phases of β-PBA, respectively.[26] The intensity of the 1726 cm^{-1} band is significantly stronger than that of the 1738 cm^{-1} band, as the PBA film cast from a solution at room temperature exhibits high crystallinity with β-crystals. In the 80/20 blend, the bands at 1738 and 1726 cm^{-1} appear at the same positions as those for neat PBA. The intensity of the 1726 cm^{-1} band over the 1738 cm^{-1} band decreases, however, apparently compared with that of neat PBA. For the 50/50 blend, the band corresponding to the amorphous PBA shifts from 1738 cm^{-1} to 1735 cm^{-1}. Moreover,

dx.doi.org/10.1021/jp110003m |J. Phys. Chem. B 2011, 115, 1950–1957

Table 1. Assignments for Major Bands Used in the Analysis of IR Spectra of PBA

position	assignment	position	assignment
910	CH_2 rocking mode in β-form crystal	909	CH_2 rocking mode in α-form crystal
930	CH_2 rocking mode in β-form crystal		
960	CH_2 rocking mode in β-form crystal	959	CH_2 rocking mode in α-form crystal
1077	C−C stretching mode in amorphous state		
1417	CH_2 bending in β-form crystal	1419	CH_2 bending in α-form crystal
1464	CH_2 bending in β-form crystal	1462	CH_2 bending in α-form crystal
1726	C═O stretching in β-form crystal	1738	C═O stretching in in amorphous state

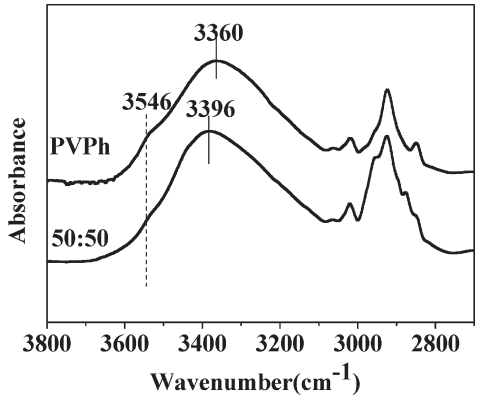

Figure 2. IR spectra in the hydroxyl stretching band region of neat PVPh and a 50/50 PBA/PVPh blend.

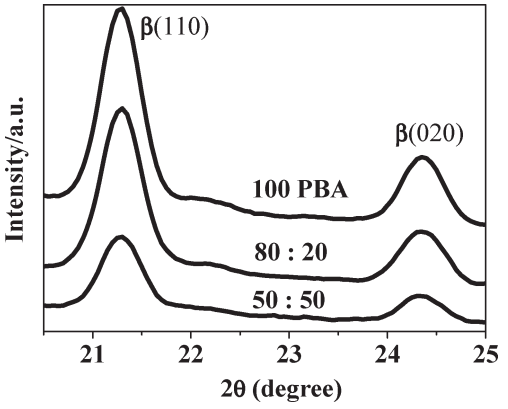

Figure 3. X-ray diffraction patterns of the spin-coating samples of neat PBA, 80/20 and 50/50 PBA/PVPh blends taken at room temperature.

a new band appears at 1708 cm^{-1}. This band is assigned to the carbonyl stretching band arising from the hydrogen bonding interaction between the carbonyl groups of PBA and the hydroxyl groups of PVPh.[28−30] Actually, this band exists already in the spectrum of the 80/20 blend, as indicated by an arrow in part b of Figure 1. It is, however, much weaker because the lower content of PVPh allows only a small amount of carbonyl groups in PBA to be involved in the hydrogen bonding. For the blend of 50/50, the disappearance of crystalline sensitive C═O stretching band at 1726 cm^{-1} and the strong absorbance of the hydrogen bonded C═O groups at 1708 cm^{-1} demonstrate unambiguously the formation of hydrogen bonding between the carbonyl group of PBA and the hydroxyl group of PVPh.

The presence of the hydrogen bonding between the carbonyl group of PBA and the hydroxyl group of PVPh has been further confirmed by analyzing the hydroxyl stretching band of PVPh. Figure 2 shows IR spectra in the region of 3800−2700 cm^{-1} of neat PVPh and the 50/50 PBA/PVPh blend. The spectrum of neat PVPh reveals two unresolved bands in the hydroxyl stretching region, corresponding to the free OH band at 3546 cm^{-1} and a broad band centered at 3360 cm^{-1} arising from the hydrogen bonded OH group (self-association). Upon blending with PBA, the intensity of the free OH band decreases, and the band corresponding to the hydrogen bonded hydroxyl group shifts to a higher wavenumber with the addition of PBA. On the basis of previous investigations,[29] these changes indicate the formation of the C═O···HO interactions, which results in a reduction of the free OH band at 3546 cm^{-1}. It should be pointed out that the broad band in the neat PVPh is more symmetrical than that in the 50/50 blend. The asymmetrical shape of the broad band in the 50/50 blend should be associated to the coexistence of both C═O···HO and HO···HO hydrogen bonds. Furthermore, the shift of broad band to the higher wavenumber in the blend is induced by the change of hydrogen bonding strength. Employing a term of the frequency difference between the free hydroxyl group and those of the hydrogen bonded hydroxyl groups as measure of the average strength of hydrogen bonding interaction,[31] it is estimated that the hydrogen bonding strength of the PBA/PVPh blend is weaker than that of the self-associated hydrogen bonding of neat PVPh. Nevertheless, hydrogen bonding between the carbonyl groups of PBA and the free hydroxyl groups of PVPh has been identified in the blend, which results in a reduction of the band intensity corresponding to the free hydroxyl groups. Moreover, taking the excellent miscibility between PBA and PVPh into account, a mixture on the molecular level is expected for an entropic ground. This may results in a situation with the PVPh molecular chains being separated and surrounded by the PBA molecular chains. In this case, the self-associated HO···HO hydrogen bonds can also be reduced.

The above experimental results indicate the development of C═O···HO hydrogen bonds in the PBA/PVPh blends. The formation of C═O···HO hydrogen bonding does, however, not affect the solution crystallization behavior of PBA, which grows always in its β-form as confirmed by the XRD of the as prepared samples. As shown in Figure 3, for all of the three samples, there are only two reflection peaks corresponding to the diffractions of the (110) and (020) lattice planes of the orthorhombic β-PBA crystals. It has been well documented that, under suitable thermal heat-treatment, the metastable orthorhombic β-form PBA is able to transit into its thermodynamically stable α-phase.[27,32,33] To follow the phase transition behavior of PBA in the PBA/PVPh blends, temperature-dependent IR spectra of PBA and its blends with PVPh were collected during the heating process. Parts a−c of Figure 4 illustrate the

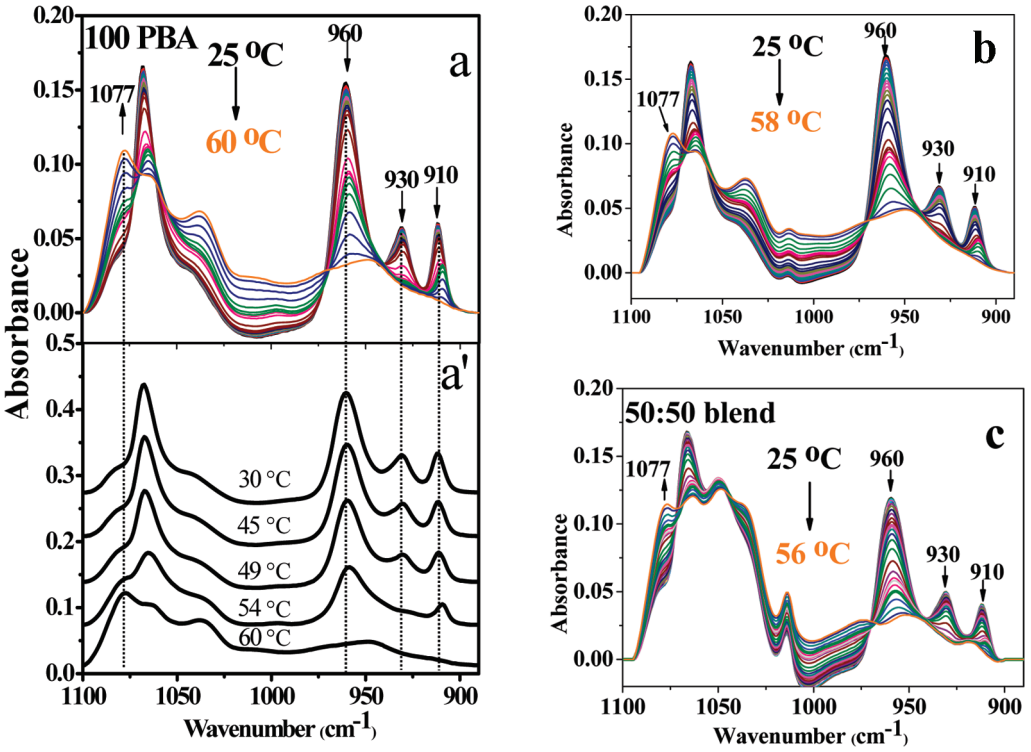

Figure 4. Temperature-dependent IR spectra in the region of 1100−890 cm^{-1} collected during the heating process of (a) neat PBA (in a′ several selected spectra are chosen and shifted for clarity), (b) the 80/20 PBA/PVPh blend, and (c) the 50/50 PBA/PVPh blend.

temperature-dependent IR spectra in the region of 1100−890 cm^{-1}. From Figure 4, it can be seen that the bands at 960, 930, and 910 cm^{-1} decrease with increasing temperature, whereas the band at 1077 cm^{-1} increases with temperature. As summarized in Table 1, the bands at 960, 930, and 910 cm^{-1} are assigned to the CH_2 rocking mode of β-PBA crystals.[33] Therefore, the 930 and 910 cm^{-1} were chosen as characteristic bands of β-PBA for monitoring the phase transition behavior of β-PBA crystals. The band at 1077 cm^{-1} due to the C−C stretching mode of amorphous PBA was selected to investigate the evolution of the chain conformation in the amorphous state during heating process. Because this band is severely overlapped with other close bands, to emphasize spectral changes during heating, the analysis of this band is performed with difference spectra obtained by subtracting the initial one from the rest of the spectra. From a′ in Figure 4, for the neat PBA, it is evident that the 930 cm^{-1} band decreases gradually with temperature and disappears completely at 54 °C. However, the bands at 960 and 910 cm^{-1} decrease and shift to lower wavenumber with temperature. This is caused by the existence of characteristic bands for α-PBA crystals located quite close to these bands, that is the 959 and 909 cm^{-1} bands for the CH_2 rocking mode of PBA in its α-form. To characterize the phase transition process of both the neat PBA and the blends, the intensity changes of the 1077, 930, and the 910 together with 909 cm^{-1} bands have been followed.

Part a of Figure 5 plots the normalized peak intensities of these bands as a function of temperature for neat PBA sample. One can clearly see that the intensity of 930 cm^{-1} band decreases first slowly and then quickly with temperature. By fitting the curve linearly, a crossover point at 47.5 °C labeled as "B", can be obtained. As the band at 930 cm^{-1} is the characteristic band of β-PBA, the temperature at which its intensity goes to zero can be regarded as the end point of β-to-α transition. Therefore, the neat PBA completes the β-to-α transition at ca. 50.7 °C. Taking this into account, the intersection "B" could be correlated to the beginning of the β-to-α transition, as it happens at sufficient high temperature (>40 °C) to provide the energy for overcoming the free energy barrier. As for the intensity changes of the IR bands in the temperature range of 27 to 47.5 °C, it may be originated from the temperature effect on the absorption behavior of β-PBA rather than the phase transition as frequently observed for many polymers during heating.

The change of the amorphous phase is characterized by monitoring the evolution of 1077 cm^{-1} band. It can be seen that, below 47.5 °C, its peak intensity keeps almost zero (the zero value indicates no change of this peak compared to the initial state as normalized peak intensity was used) with temperature, indicating the maintenance of PBA crystallinity. Thereafter, a significant intensity increase of 1077 cm^{-1} band indicates an increment of the amorphous phase. Same crossover point of 47.5 °C is also obtained from the plot of the normalized intensity of 1077 cm^{-1} band, reflecting the occurrence of phase transition. The intensity increase of the amorphous band during phase transition may be attributed either to the melting of the PBA β crystals before phase transition or to the segment conformation change of the PBA chains during the phase transition. It is known that the PBA α crystal has a monoclinic unit cell with axially compressed planar zigzag conformation, whereas the β crystal possesses an orthorhombic unit cell with all-trans conformation. This means that the phase transition is realized through the axial compression of the PBA chain segments. During this process, there may be an intermediate state, in which the PBA chains in the β-phase have lost their conformation before related α-crystal chain conformation forms.

For the 910 cm^{-1} band, its intensity also decreases slowly during heating from 27 to ca. 47.5 °C and then is followed by an

dx.doi.org/10.1021/jp110003m |J. Phys. Chem. B 2011, 115, 1950–1957

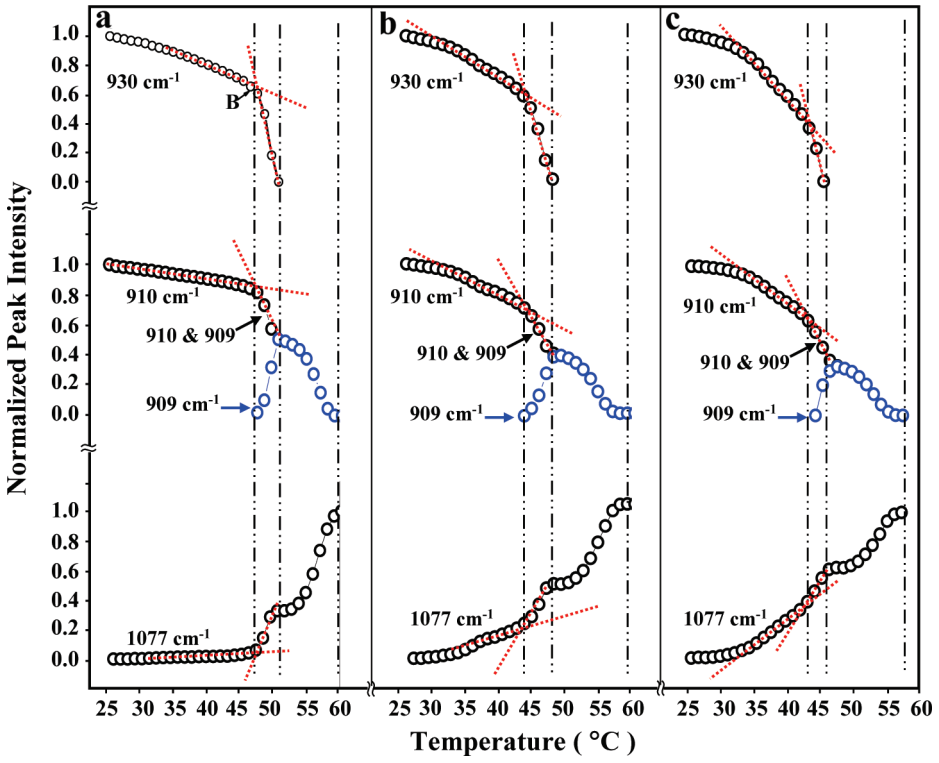

Figure 5. Plots of normalized peak intensity of the crystalline sensitive bands at 930, 910, and 909 cm^{-1}, and the amorphous sensitive band at 1077 cm^{-1} as a function of temperature in neat PBA (a) and the 80/20 (b) and 50/50 blends (c). The 910 and 909 cm^{-1} bands coexist in the phase transition region. The 909 cm^{-1} band for the α-PBA crystals in this region is separated from the overall band of both 910 and 909 cm^{-1}.

abrupt intensity decrease. A crossover point at 47.5 °C is obtained. It should be pointed out that, however, the intensity of the 930 cm^{-1} band decreases gradually to zero in the process of phase transition from 47.5 to 50.7 °C, whereas the band at around 910 cm^{-1} still exists above 50.7 °C. This arises from the fact that the 910 cm^{-1} is a crystallization sensitive band for β-PBA crystals, whereas the band at 909 cm^{-1} is the crystallization sensitive band for their α-counterparts. These two peaks can be well recognized before and after complete phase transition, see spectra at 30 and 54 °C shown in a′ of Figure 4. During the phase transition, because of the severe overlap of these two bands, the band appeared around this position should correspond to the newly created α and the untransited β PBA crystals. In other words, its intensity is the sum of $I_{\beta 910}$ and $I_{\alpha 909}$, that is $I_{total} = I_{\alpha 909} + I_{\beta 910}$. Before the phase transition, a purely β phase leads to $I_{total} = I_{\beta 910}$, whereas after the transition, the disappearance of β phase leads to $I_{total} = I_{\alpha 909}$. To follow the change of α-PBA crystals during β-to-α conversion process, a separation of the $I_{\alpha 909}$ from the I_{total} is necessary. To this end, the following procedure was used. As the 930 cm^{-1} band is only associated with the β-PBA phase, $I_{\beta 910}$ can be derived from I_{930} by $I_{\beta 910} = KI_{930}$, where K represents the coefficient reflecting the relationship between $I_{\beta 910}$ and I_{930}. For pure β phase, K can be easily determined by $K = I_{\beta 910}/I_{930} = I_{910}/I_{930}$. If K is a constant, then $I_{\beta 910}$ during phase transition can be easily obtained from the I_{930} value. It was found that the K value is temperature dependent even before the phase transition. Figure 6 shows a plot of K vs T for T < 47.5 °C, which is assumed as the onset phase transition temperature of the PBA β crystals. The curve can be well described by an exponential equation as:

$$K = 0.00237 \times \exp(T/9.45) + 0.961 \quad (1)$$

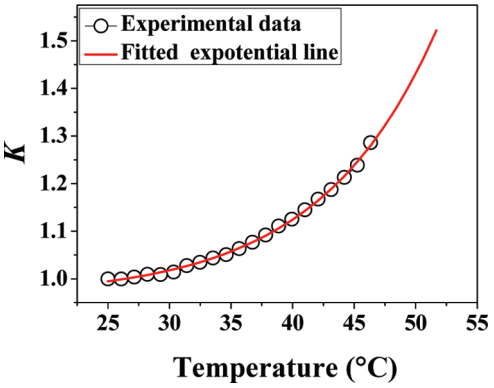

Figure 6. Normalized peak intensity ratio of two bands at 910 and 930 cm^{-1} (K) in the temperature window of 25 to 47.5 °C with the fitted line based on an exponential equation.

Assuming the temperature dependence of the K value within the phase transition temperature window of 47.5 °C < T < 50.7 °C follows the same law, it can be then deduced from the fitted line as a standard curve. In this way, the $I_{\alpha 909}$ during the phase transition can be obtained from:

$$I_{\alpha 909} = I_{total} - I_{\beta 910} = I_{total} - KI_{930} \quad (2)$$

The normalized peak intensity of $I_{\alpha 909}$ is presented in Figure 5 as the blue circles. It can be seen that the α phase content increases simultaneously along with the decrease of β phase content. It reaches maximum at 50.7 °C, indicating the completion of β-to-α transition.

dx.doi.org/10.1021/jp110003m |J. Phys. Chem. B 2011, 115, 1950–1957

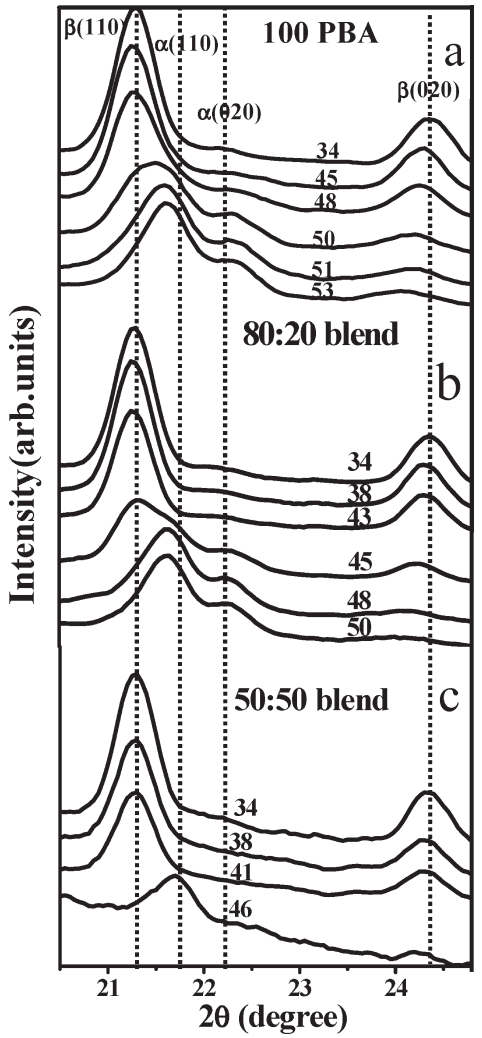

Figure 7. X-ray diffraction patterns of PBA as a function of temperature in (a) the neat PBA, (b) 80/20 PBA/PVPh blend, and (c) the 50/50 PBA/PVPh blend.

From the above experimental results, it is concluded that the β-to-α transition of pure PBA starts at 47.5 °C and completes at 50.7 °C. To find out the validity of this conclusion reached from the IR results, especially those for the onset temperature of phase transition process, a temperature-dependent XRD measurement was performed for neat PBA. Part a of Figure 7 shows its temperature-dependent XRD patterns. It is clear from part a of Figure 7 that the as-prepared sample exhibits only the (110) and (020) reflections of the β-PBA crystals. During the heating process, no detectable change in the XRD pattern of PBA can be found below 46 °C, indicating that the β-PBA crystals remain stable below this temperature. When the sample is heated to 48 °C, the coexistence of diffraction peaks associated to the (110) lattice planes of both β and α crystals demonstrates the occurrence of the β-to-α transformation. Over 51 °C, the appearance of only (110) and (020) diffractions corresponding to the α-form PBA crystals indicates the completion of the β-to-α transition. The XRD patterns then remain unchanged in the temperature window of ~51−53 °C. Further heating of the sample results in the disappearance of all diffraction peaks caused by melting of the PBA crystals. By comparing, it can be found that the XRD and IR results are in good agreement.

For the 80/20 PBA/PVPh blend, the evolution trends of the IR bands are somewhat different from those of the neat PBA. As can be seen from part b of Figure 5, the intensities of the IR bands at 930, 910, and 1077 cm^{-1} display clearly multistage alterations. The first stage ends around 34 °C. In this stage, the intensities of the 930 and 910 cm^{-1} bands decrease while the intensity of the 1077 cm^{-1} band increases slightly in the similar ways as that observed for neat PBA due to the temperature effect on the absorption coefficient. The second stage completes at about 44.7 °C. In this second stage, accelerated intensity decreases of the 930 and 910 cm^{-1} bands and an accelerated intensity increase of the 1077 cm^{-1} band are clearly demonstrated. Then, abrupt intensity changes of these bands are seen in a narrow temperature window of 45−48 °C, which corresponds to the third stage. Thereafter, the intensity changes of these bands are again similar to that of the neat PBA. One may correlate both the second and third stages to the β-to-α phase transition with different transition rates. This is actually not the case when the $I_{\alpha 909}$ deduced from the above proposed way for pure PBA is analyzed. As presented in part b of Figure 5, no 909 cm^{-1} band for the α-PBA crystals can be identified below 44.7 °C, indicating that no β-to-α transition takes place at all. The appearance and abrupt intensity increase of the 909 cm^{-1} band for the α-PBA crystals within the temperature range of 44.7−48 °C indicate that the phase transition starts actually at about 44.7 °C and completes at about 48 °C, namely corresponding to the third stage. This has been further confirmed by X-ray diffraction, which will be discussed in the next paragraph. The accelerated intensity changes in the second stage may be caused by different environment of ordered conformational segments as observed for many polymers. Moreover, the XRD results shown in Figure 7 suggests the melting of some β-PBA crystals, which should also contributes to some extent of the accelerate IR intensity changes in the second stage.

It was found that the XRD pattern of the PBA/PVPh film keeps almost unchanged below 34 °C, indicating that the β-PBA crystals remain unchanged with almost the same crystallinity. In the temperature window of 34−43 °C, as shown in the part b of Figure 7, the diffractions in the XRD pattern of the PBA/PVPh film are still accounted to the β-PBA crystals but with slight decrease in the peak intensities. This indicates the melting of some β-PBA crystals, which results in accelerated intensity changes of the IR bands. The appearance of the (110) and (020) reflections of the α-PBA as well as the β-PBA crystals are observed in the temperature range above 45 °C but below 47 °C, demonstrating that the phase transition takes place in this temperature range. The phase conversion is found to be finished at 48 °C because only reflections of the α-PBA crystals are observed above this temperature. The XRD results indicate that the β-to-α phase transition occurs in the narrow temperature window of 44.7−48 °C, which corresponds to the abrupt intensity changes of the IR bands, that is, the third stage. This is in good accordance with the IR analysis on the 909 cm^{-1} band of the α-PBA crystals. Combining the IR and X-ray results, it is clear that blending PBA with PVPh results in an earlier start of the β-to-α phase transition of PBA crystals. Moreover, the accelerated intensity changes of the IR bands at 910, 930, and 1077 cm^{-1} in the second stage are identified. All of these changes reflect the influence of PVPh on PBA and are more evidently revealed by the 50/50 PBA/PVPh blend.

As presented in the part c of Figure 5, the plots of normalized peak intensities of the IR bands exhibit clearly multistage

Table 2. Characteristic Temperatures (°C) of PBA during the Heating Process

	onset phase transition temperature	end phase transition temperature	melting temperature of the α PBA
neat PBA	47.5 °C	50.7 °C	60 °C
80:20			
PBA/PVPh	44.7 °C	48.0 °C	57 °C
50:50			
PBA/PVPh	42.8 °C	45.2 °C	55 °C

changes. The stage corresponding to the β-to-α transition, that is the third stage, falls approximately in the temperature range of 43−45.2 °C. This indicates an even earlier start of the β-to-α transition. After the phase transition, the produced α-PBA crystals are stable in a short time period and soon start to melt as deduced from the intensity decrease of the 909 cm^{-1} band and the intensity increase of the 1077 cm^{-1} band.

According to the above results, the influence of PVPh on the phase transition behavior of PBA can be discussed. We summarize the onset and end temperature of β-to-α phase transition and the melting temperature of the resultant α phase for the neat PBA and its blends in Table 2. There are clearly depressions of β-to-α phase transition temperature of the β-PBA and melting temperature of the resultant α PBA with the addition of PVPh. The melting temperature depression of a crystalline polymer blended with an amorphous polymer is a general phenomenon for the miscible systems and has been well explained based on the Flory−Huggins theory.[34,35] Taking the excellent miscibility of PBA with PVPh into account, the decrease in melting temperature of the PBA crystals is easily to be understood. As for the phase transition temperature depression, it is reasonable to assume that the melting temperature depression is valid not only to the α but also to β PBA crystals. From this point of view, it is highly speculated that the β-to-α phase transition takes place through a microdomain melting and recrystallization process.

Another thing, which should be addressed, is the accelerated intensity decrease of the crystalline sensitive IR bands and the accelerated intensity increase of the amorphous sensitive IR band in the second stage of the blend systems. The formation of hydrogen bonding between the PBA and PVPh has been clearly demonstrated. The hydrogen bonding interaction will unambiguously influence the crystallization of PBA. Imperfect PBA crystals in the PBA/PVPh blends with poor thermal stability are expected to be created, which can melt at relatively lower temperature and, therefore, result in IR spectra changes before the phase transition. However, morphological changes induced by addition of PVPh, such as lamellar thickness, and crystal orientation of the PBA in the blends may also influence the thermal behavior of the PBA. A correlation between the morphology of the PBA/PVPh blend and the phase transition behavior is now under study.

CONCLUSIONS

The phase transition behavior of polymorphic PBA crystals in the PBA/PVPh blends with different blend ratios has been investigated by use of IR and XRD. It has been found that a hydrogen bonding is developed between the C═O group of PBA and the OH group of PVPh. The formation of hydrogen bonding does not influence the solution crystallization behavior of PBA and the β PBA crystals are formed in all solution cast samples. They influence, however, the phase transition of β-PBA crystals. It was found that with increasing PVPh content in the PBA/PVPh blends, the β-to-α phase transformation temperature decreases evidently. The influence of PVPh on the thermal behavior of the PBA crystals is also revealed by the different intensity alternations of the IR bands even before the occurrence of phase transformation. Unlike the neat PBA sample, in which the crystalline and amorphous IR bands changes gradually with temperature before phase transtion, multistage alterations of the intensities of IR bands in the heating process before phase transition are observed in the blend samples. It is caused by the melting of the imperfect β-PBA crystals resulting from the addition of PVPh.

AUTHOR INFORMATION

Corresponding Author

*E-mail: suikyo@kwansei.ac.jp (I.T.); skyan@mail.buct.edu.cn, Tel: +81-79-565-9722, Fax: +81-79-565-9077 (S.Y.).

ACKNOWLEDGMENT

This study was financially supported by Kwansei Gakuin University (Kwansei Gakuin University Joint Research Fund, 2009), and the National Natural Science Foundations of China (No. 21004003). We would like to thank Prof. Takeji Hashimoto for valuable discussions.

REFERENCES

(1) Lu, C.; Chen, X.; Xie, Z.; Lu, T.; Wang, X.; Ma, J.; Jing, X. *Biomacromolecules* **2006**, *7*, 1806.
(2) Zhang, J.; Jiang, L.; Wolcott, M.; Zhang, J. *Biomacromolecules* **2006**, *7*, 199.
(3) Guo, Q.; Kinight, P.; Wu, J.; Muther, P. *Macromolecules* **2010**, *43*, 4991.
(4) Ryan, A. J. *Nat. Mater.* **2002**, *1*, 8.
(5) Pernot, H.; Baumert, M.; Court, F.; Leibler, L. *Nat. Mater.* **2002**, *1*, 54.
(6) Jeon, H. K.; Kim, J. K. *Macromolecules* **2000**, *33*, 8200.
(7) Cigana, P.; Favis, B. D.; Albert, C.; VuKhanh, T. *Macromolecules* **1997**, *30*, 4163.
(8) Xue, M. L.; Yu, Y. L.; Sheng, J.; Chuah, H. H.; Geng, C. H. *J. Macromol. Sci., Phys.* **2005**, *B44*, 317–329.
(9) Kim, H. Y.; Ryu, D. Y.; Jeong, U.; Kho, D. H.; Kim, J. K. *Macromol. Rapid Commun.* **2005**, *26*, 1428.
(10) Asari, T.; Matsuo, S.; Takano, A.; Matsushita, Y. *Macromolecules* **2005**, *38*, 8811.
(11) He, Y.; Zhu, B.; Inoue, Y. *Prog. Polym. Sci.* **2004**, *29*, 1021.
(12) Hexig, B.; He, Y.; Asakawa, N.; Inoue, Y. *J. Polym. Sci., Part B: Polym. Phys.* **2004**, *42*, 2971.
(13) Viswanathan, S.; Dadmun, M. D. *Macromolecules* **2003**, *36*, 3196–3205.
(14) Duan, Y. Z.; Pearce, E. M.; Kwei, T. K.; Hu, X. S.; Rafailovich, M.; Sokolov, J.; Zhou, K. G.; Schwarz, S. *Macromolecules* **2001**, *34*, 6761.
(15) Park, T.; Zimmerman, S. C. *J. Am. Chem. Soc.* **2006**, *128*, 11582.
(16) Kushner, A. M.; Vossler, J. D.; Williams, G. A.; Guan, Z. *J. Am. Chem. Soc.* **2009**, *131*, 8766.

(17) Moskala, E. J.; Howe, S. E.; Painter, P. C.; Coleman, M. M. *Macromolecules* **1984**, *17*, 1671.
(18) Pedrosa, P.; Pomposo, J. A.; Calahorra, E.; Cortazar, M. *Polymer* **1995**, *36*, 3889.
(19) Iriondo, P.; Iruin, J. J.; Fernandez-Berridi, M. J. *Polymer* **1995**, *36*, 3235.
(20) Zhang, L.; Goh, S. H.; Lee, S. Y. *J. Appl. Polym. Sci.* **1999**, *74*, 383.
(21) Zhang, L.; Goh, S. H.; Lee, S. Y. *Polymer* **1998**, *39*, 4841.
(22) Qiu, Z. B.; Komura, M.; Ikehara, T.; Nishi, T. *Polymer* **2003**, *44*, 8111.
(23) Minke, R.; Blackwell, J. *J. Macromol. Sci., Phys.* **1979**, *B16*, 407.
(24) Minke, R.; Blackwell, J. *J. Macromol. Sci., Phys.* **1980**, *B18*, 233.
(25) Gan, Z.; Kuwabara, K.; Abe, H.; Iwata, T.; Doi, Y. *Polym. Degrad. Stab.* **2005**, *87*, 191.
(26) Yan, C.; Zhang, Y.; Hu, Y.; Ozaki, Y.; Shen, D.; Gan, Z.; Yan, S.; Takahashi, I. *J. Phys. Chem. B* **2008**, *112*, 3311.
(27) Gan, Z.; Kuwabara, K.; Abe, H.; Iwata, T.; Doi, Y. *Biomacromolecules* **2004**, *5*, 371.
(28) Yang, F.; Qiu, Z.; Yang, W. *Polymer* **2009**, *50*, 2328.
(29) Lee, L.; Woo, E. M.; Chen, W.; Chang, L.; Yen, K. *Colloid Polym. Sci.* **2010**, *288*, 439.
(30) Belflore, L. A.; Qin, C.; Ueda, E.; Pires, A. *J. Polym. Sci., Part B: Polym. Phys.* **1993**, *31*, 409.
(31) Moskala, E. J; Varnell, D. F.; Coleman, M. M. *Polymer* **1985**, *26*, 228.
(32) Gan, Z.; Abe, H.; Doi, Y. *Macromol. Chem. Phys.* **2002**, *203*, 2369.
(33) Yang, J.; Li, Z.; Pan, P.; Zhu, B.; Dong, T.; Inoue, Y. *J. Polym. Sci., Part B: Polym. Phys.* **2009**, *47*, 1997.
(34) Flory, P. J. *Principles of Polymer Chemistry*; Ithaca, NY: Cornell University Press, 1953.
(35) Nishi, T.; Wang, T. T. *Macromolecules* **1975**, *8*, 909.